

## Workability and mechanical properties of ultrasonically cast Al–Al<sub>2</sub>O<sub>3</sub> nanocomposites

Suhrit Mula<sup>a,d,\*</sup>, S.K. Pabi<sup>d</sup>, Carl C Koch<sup>b</sup>, P. Padhi<sup>c</sup>, S. Ghosh<sup>d</sup>

<sup>a</sup> Metallurgical and Materials Engineering Department, National Institute of Technology, Rourkela 769 008, India

<sup>b</sup> Department of Materials Science and Engineering, NC State University, Raleigh NC 27695, USA

<sup>c</sup> Konark Institute of Science and Technology, Bhubaneswar 752 050, India

<sup>d</sup> Metallurgical and Materials Engineering Department, Indian Institute of Technology, Kharagpur 721 302, India

### ARTICLE INFO

#### Article history:

Received 15 January 2012

Received in revised form

15 June 2012

Accepted 10 August 2012

Available online 17 August 2012

#### Keywords:

Nanocomposite

Workability

Nanoindentation hardness

Dislocation

Transmission electron microscopy (TEM)

### ABSTRACT

Workability and mechanical properties of the ultrasonically cast Al–X wt% Al<sub>2</sub>O<sub>3</sub> (X=2, 3.57 and 4.69) metal matrix nanocomposites were reported in the present investigation. The Al–Al<sub>2</sub>O<sub>3</sub> (average size ~10 nm) composites showed maximum reduction ratios of 2, 1.75 and 1.41 at room temperature, and 8, 7 and 6 at 300 °C. The elastic modulus, nanoindentation hardness, microhardness and Vickers hardness were measured on the as-cast, cold and hot rolled specimens. The tensile properties were also evaluated for the as-cast composites for different wt% of reinforcement. The microstructural examination was done by optical, scanning and transmission electron microscopy. The strength and workability of the nanocomposites were discussed in the light of dislocation/particle interaction, particle size and its concentration, inter-particle spacing and working temperature. 2 wt% of Al<sub>2</sub>O<sub>3</sub> reinforcement showed better combination of workability and mechanical properties possibly due to better distribution of particulates in the matrix.

© 2012 Elsevier B.V. All rights reserved.

### 1. Introduction

Researchers are, recently, turning to particulate-reinforced aluminum-metal matrix composites (AMCs) because of their high strength to weight ratio, long fatigue life, and improved thermal stability, low cost and reasonably isotropic properties [1–4] especially in those applications, where extreme loading or thermal conditions are not required. Besides, the mechanical properties the workability of AMCs is essential for the fabrication of any component for practical uses, such as automotive components, transportation and construction. Composite's ability to be easily shaped is known as workability. Generally, the workability index (WI) has been positively affected by decreasing particulate size and volume fraction [5].

Aluminum and most of its alloys are known to have high degree of deformability. It can be thinned down to form sheet in mm level and even thinner to micron level thin foil by rolling. Aluminum or aluminum alloys reinforced with particulates enhance the mechanical strength but on the sacrifice of ductility. Normally, the ductility of the composites deteriorates with high ceramic particle concentration [6] with micron size particles. To maintain the good ductility [7] as well as strength, it is very much

interesting to use nano-sized ceramic particles to strengthen the metal matrices, so-called metal matrix nano-composite (MMNC). Bulk composite reinforced with nano-sized ceramic particulate can be developed by special casting techniques such as ultrasonic casting [8–10]. The difficulty in the casting process is that cast composite obtained in the shape of ingot. Therefore, deformation processing or workability of composite is very much important in modern technology to obtain useful shapes such as sheets, tubes and rods etc. The problems encountered during plastic deformation of particle reinforced composites are cracking and particle fracture, flow instability and localization creating non-uniform structure. The casting defects such as blowhole and porosity in a cast ingot are eliminated by hot rolling or hot forging to the improvement of the mechanical properties such as ductility and fracture toughness etc. In this regard, rolling is the most widely used metal working process because of it lends itself to high production and close control of the final product [11]. Cold working of materials increases strength or hardness, saving cost of forming with better surface finish of the products; whereas, hot working is necessary so that large strains can be achieved with essentially no strain hardening.

Therefore, it is essential to evaluate the workability as well as other mechanical properties of the nanocomposites developed by ultrasonic casting in the present investigation. Cold (at room temperature) and hot rolling (at 300 °C) were carried out on the as-cast Al–X wt% Al<sub>2</sub>O<sub>3</sub> (X=2, 3.57 and 4.69) nanocomposites to

\* Corresponding author. Tel.: +91 661 2462565; fax: 91 661 2472926.  
E-mail address: [suhritmula@gmail.com](mailto:suhritmula@gmail.com) (S. Mula).

determine their workability. Mechanical properties, namely, microhardness, nanoindentation hardness and tensile strength were also investigated.

## 2. Experimental

Micron sized (avg.  $\sim 75 \mu\text{m}$ )  $\text{Al}_2\text{O}_3$  powder (Loba Chemie) was ball milled in a Fritsch Pulverisette-5 planetary ball mill for 22 h to produce nanosized (average size  $\sim 10 \text{ nm}$ )  $\text{Al}_2\text{O}_3$  dispersoids. The mill was operated at 300 rpm with a tungsten carbide grinding media, and toluene was used as the process control agent. The ball to powder weight ratio was maintained at 10:1. The particle size of the milled  $\text{Al}_2\text{O}_3$  powder was investigated by transmission electron microscopy analysis (JEOL JEM-2100). Commercially pure Al (cp-Al) having a nominal composition of Al–0.96% Fe–0.43% Mg–0.26% Si was reinforced with this nanosized ( $< 10 \text{ nm}$ )  $\text{Al}_2\text{O}_3$  to prepare the cast ingots of Al– $\text{Al}_2\text{O}_3$  nanocomposites with 2, 3.57 and 4.69 wt% of reinforcement by a non-contact ultrasonic method [12]. Cold rolling of the sliced cast ingots was successfully carried out up to a maximum workability index (WI) (=initial height/final height) of 2, 1.75 and 1.41 for 2, 3.57 and 4.69 wt%  $\text{Al}_2\text{O}_3$  reinforced composites, respectively, whereas, hot rolling of the respective material showed a maximum WI of 8, 7 and 6.

Nanoindentation tests were conducted using an MTS-XP nanoindenter to evaluate nanoindentation hardness and elastic modulus of the nanocomposites. A Leica 550 MW tester was used for microhardness test as per ASTM E92-82 standard using 5 g load with 15 s dwell time and an indenter speed of  $25 \mu\text{s}$ . Vickers hardness tester (Fritz Heckert, Germany) was used to determine Vickers hardness values of composites using 15 kg load with a dwell time of 50 s. Tensile tests of the cast materials were carried out by a Tinius Olsen H50KS tester with a crosshead velocity of 1 mm/min. Tensile specimens were prepared as per ASTM E8 standard. Each data of the tensile strength measurement was the average of five tests.

Microstructural characterization of the Al– $\text{Al}_2\text{O}_3$  nanocomposites was carried out using optical microscope (Leica DMLM), scanning electron microscope (JEOL JSM-6480 LV) and JEOL JEM-2100 transmission electron microscope (TEM).

## 3. Results and discussion

The particle size of the ball milled powder was determined by TEM study. Fig. 1 shows the TEM micrograph of  $\text{Al}_2\text{O}_3$  powder milled for 22 h. The average particle size could be estimated about  $\sim 10 \text{ nm}$  (Fig. 1). The powder particles were agglomerated because of high surface energy of the nanosized particles. The ball milled nano powders were used to prepare Al–2%  $\text{Al}_2\text{O}_3$ , Al–3.57%  $\text{Al}_2\text{O}_3$  and Al–4.69%  $\text{Al}_2\text{O}_3$  composites by the non-contact ultrasonic method [12]. The approximate grain size and possible distribution of the particles in the as-cast composites can be ascertained from the optical and SEM micrographs (Fig. 2(a) and (b)) of Al–2%  $\text{Al}_2\text{O}_3$  composite. The enclosed regions in the micrograph delineated Al grains sizes varying from as low as  $40 \mu\text{m}$  to as high as  $75 \mu\text{m}$ . A clear idea about the  $\text{Al}_2\text{O}_3$  particle size and their dispersion can be obtained from the TEM micrograph (Fig. 2(c)) of the as-cast Al–2%  $\text{Al}_2\text{O}_3$  composite. The details of the microstructural features of Al–2%  $\text{Al}_2\text{O}_3$  composite were reported earlier in [12].

The cast composites with different wt% of reinforcement were investigated for mechanical properties by nanoindentation test, Vickers hardness test and tensile test. The elastic modulus and hardness of composites were compared with conventionally cast

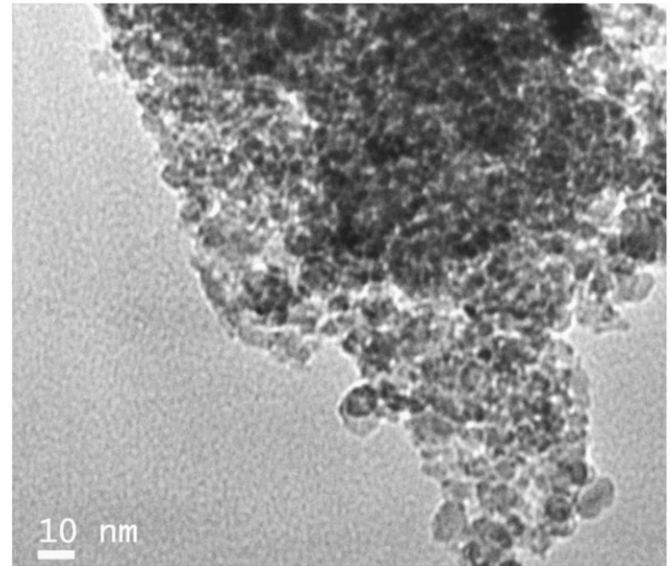
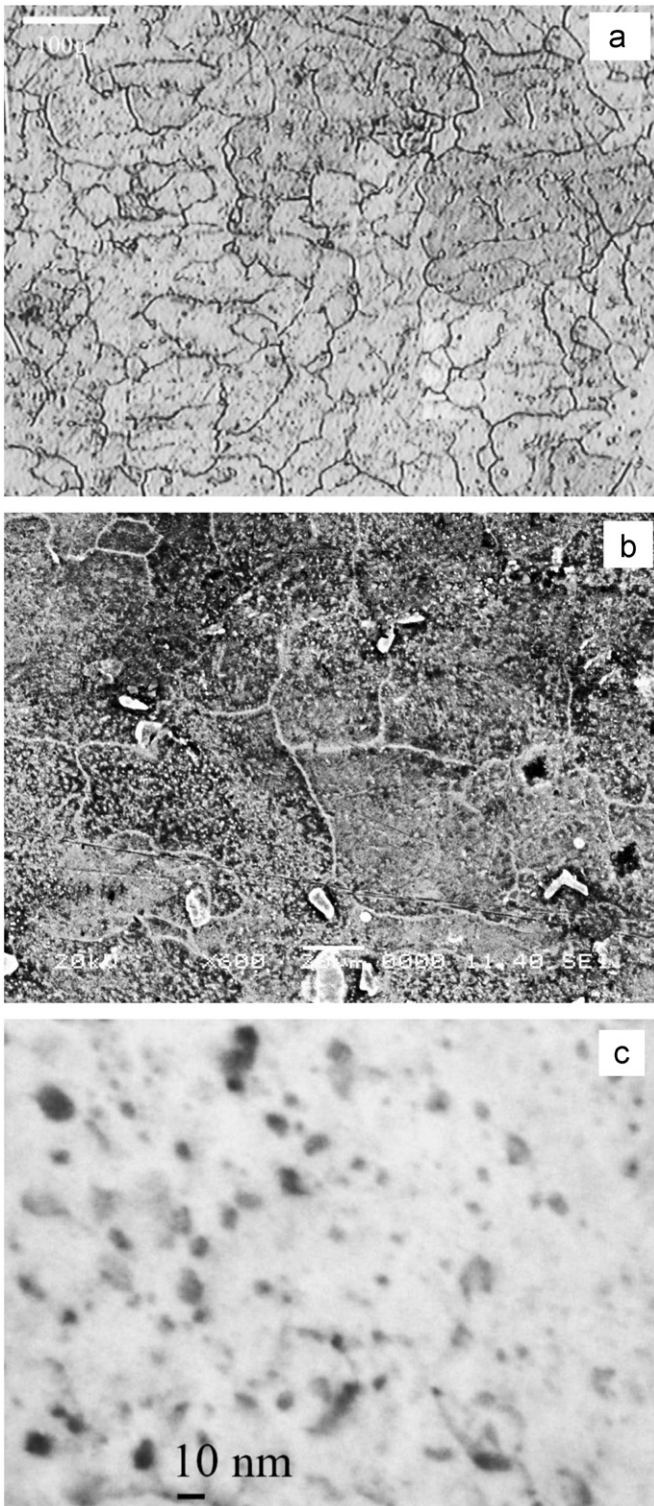


Fig. 1. TEM micrograph of  $\text{Al}_2\text{O}_3$  powder milled for 22 h showing the agglomerated form of nanoparticles.

and ultrasonically cast cp-Al without reinforcement as shown in Table 1. Each data of nanoindentation hardness and elastic modulus reported here was a statistical mean from measurements on 40 locations. The results showed that the elastic modulus of ultrasonically cast cp-Al was marginally higher ( $\sim 4.8\%$ ) than the conventionally cast cp-Al. Reinforcement with 2%  $\text{Al}_2\text{O}_3$  resulted in  $\sim 3.6\%$  increase in the elastic modulus than the ultrasonically cast cp-Al. Further increased in reinforcement to 3.57% and 4.69%, the elastic modulus was enhanced by another 4% and 5.5%, respectively, compared to 2%  $\text{Al}_2\text{O}_3$  reinforced composite. The elastic modulus of the metals and alloys is not quite sensitive to the structural features like grain size, point defects and dislocation density etc. [11]. It was also interesting to note from Table 1, that the standard deviation values in the measured elastic modulus were much higher in case of nanocomposites, as compared to ultrasonically cast cp-Al. The highest variation of elastic modulus was observed for 4.69% reinforced composite. This is possibly due to increased in the heterogeneity and clustering tendency of the particulates in the matrix with increasing amount of reinforcement.

Table 1 clearly shows that the hardness is very much sensitive to the structural changes in the Al matrix and the composite. The average hardness of cp-Al measured by conventional Vickers hardness test showed a good agreement with the average microhardness and nanoindentation hardness of the as-cast samples. Grain refinement by ultrasonic casting in cp-Al without reinforcement resulted in  $\sim 42\%$  increase in the nanoindentation hardness and microhardness, as well as, Vickers hardness (Table 1). Reinforcement of cp-Al matrix by 2%  $\text{Al}_2\text{O}_3$  nano-dispersoids resulted in  $\sim 100\%$  enhancement in the Vickers hardness and microhardness compared to that of ultrasonically cast cp-Al. With further increased in the reinforcement, the overall hardness values of the composites was increased by  $\sim 16\%$  for 3.57% and  $\sim 29\%$  for 4.69% reinforcement, respectively, compared to that of 2%  $\text{Al}_2\text{O}_3$  reinforced composite. It is to be noted that, the load dependent hardness is not realized in the present study, although hardness is load dependent in the micro and nanoindentation regime due to indentation size effect (ISE) [13]. In the present study, the hardness measured by Vickers hardness, microhardness and nanoindentation tests showed very close data, and ISE is not clearly revealed. This issue is to be investigated separately in our forthcoming study.



**Fig. 2.** (a) Optical, (b) SEM and (c) bright field TEM micrographs of cast Al-2% Al<sub>2</sub>O<sub>3</sub> nanocomposite.

Fig. 3 show (a) typical load–displacement curve and (b) hardness vs. displacement plots during nanoindentation for Al-2% Al<sub>2</sub>O<sub>3</sub> nanocomposite. Fig. 3(a) clearly indicates that load on sample gradually increases with the penetration depth and reaches the maximum applied load of 50 mN, where depth of indentation was approximately 400 nm. The calculation range was ascertained from the horizontal portion of the hardness vs. indentation depth curves.

The typical range of calculation for hardness was 100–300 nm indentation depth as shown in Fig. 3(b). The same has been followed to estimate elastic modulus also.

Fig. 3(c) shows the graphical representation of the variation of nanoindentation hardness (converted to  $H_v$  as per the formulae: Derived  $H_v$  in Vickers scale =  $92.65 \times$  nanoindentation hardness  $H$  (GPa) [14]) and elastic modulus of Al–Al<sub>2</sub>O<sub>3</sub> nanocomposites with increasing weight percentage of Al<sub>2</sub>O<sub>3</sub>. It shows that the elastic modulus increases with increase in the reinforcement, but the increment is small, as shown in Fig. 3(c). On the other hand, increase in the hardness is more pronounced with the increase in the reinforcement. In both cases, standard deviation values increased with increase in the reinforcement, which indicated increase in the heterogeneity of the microstructures of the nanocomposites.

Nevertheless, the standard deviation values in nanoindentation hardness is found to be much higher in case of 4.69% Al<sub>2</sub>O<sub>3</sub> reinforced composite compared to the other two compositions due to the microscopically increased in the heterogeneity of the structure with increasing volume fraction of particulates. Therefore, the statistical data from the nanoindentation measurement suggested that more uniform distribution was required for the composite reinforced with higher volume fraction of particulates.

Tensile strength of the cast materials of Al–X wt% Al<sub>2</sub>O<sub>3</sub> ( $X=0, 2, 3.57$  and  $4.69$ ) compositions were assessed by a Tinius Olsen H50KS tensile tester with a crosshead velocity of 1 mm/min. The tensile specimens were prepared as per ASTM E8 standard as shown in Fig. 4(a) and the results reported here are based on testing of five samples for each. Fig. 4(b) shows the comparison of engineering stress–engineering strain curves of ultrasonically cast cp-Al and cast composites. A pronounced improvement in the yield strength (YS) and ultimate tensile strength (UTS) was observed for the 2% Al<sub>2</sub>O<sub>3</sub> reinforced composite with a nominal reduction in % elongation, compared to that of ultrasonically cast cp-Al. The observed YS and UTS of ultrasonically cast cp-Al and composite were 30 MPa and 62 MPa, respectively and those of 2% Al<sub>2</sub>O<sub>3</sub> reinforced composite were 47 MPa and 91.6 MPa, respectively. The nanocomposite showed an increase in YS by 56.7% and UTS by 47.7% with a marginal reduction in ductility compared to ultrasonically cast cp-Al without reinforcement. The % elongation of the ultrasonically cast cp-Al was ~50%, and this, as anticipated, diminished to 41% in case of the composite. The improvement in tensile strength of the other two composites were also compared and presented in the same figure, i.e. Fig. 4(b). It showed a slight increase in tensile strength for 3.57 and 4.69% Al<sub>2</sub>O<sub>3</sub> reinforced composites with sufficient reduction of ductility compared to that of ultrasonically cast cp-Al. The % elongations of 3.57% and 4.69% particulate reinforced composites reduced to 36% and 34%, respectively, with corresponding UTS of 93 MPa and 96 MPa.

Fig. 5 shows the variation of flow stress with wt% of reinforcement for different strain levels. It can be seen from Fig. 5 that 2% Al<sub>2</sub>O<sub>3</sub> reinforcement resulted in significant increase in the stress level. But, further addition of the reinforcement, in excess of 2%, increased the stress, but not a significant amount. It can also be observed that the variation of stress with increase in the reinforcement beyond 2% is almost linear. Fig. 5 also shows that for a particular wt% of reinforcement the stress level increases with increase in the strain.

Ability of the material to be easily shaped is known as workability. A workability index (WI) can be defined as the height of the original specimen ( $H_0$ ) divided by its final height after deformation ( $H$ ), i.e.  $H_0/H$ . Generally, the workability index (WI) has been positively affected by decreasing particulate size and volume fraction. Maximum WI can be taken for maximum possible reduction just before cracking due to plastic deformation. As deformation increases, the final specimen height decreases and

**Table 1**  
Comparison of elastic modulus and hardness with variation of wt% of Al<sub>2</sub>O<sub>3</sub> reinforcement in cp-Al.

	cp-Al	uc <sup>a</sup> Al–Al <sub>2</sub> O <sub>3</sub> nanocomposites			
Reinforcement (%)	–	0	2	3.57	4.69
Nanoindentation					
Elastic modulus <i>Y</i> (GPa)	69.3 ± 1.7	72.6 ± 1.5	75.2 ± 2.0	78.5 ± 2.9	79.4 ± 3.5
Nanoindentation hardness <i>H</i> (GPa)	0.35 ± 0.02	0.54 ± 0.01	1.05 ± 0.04	1.37 ± 0.09	1.52 ± 0.15
Derived <i>H<sub>v</sub></i> <sup>b</sup> (from <i>H</i> value in GPa)	32.5	50.0	97.3	126.9	140.8
Vickers hardness ( <i>H<sub>v</sub></i> )	36	51	102.0	127	149
Microhardness ( <i>H<sub>v</sub></i> )	37	52	100.0	126	146

<sup>a</sup> uc stands for ultrasonically cast.

<sup>b</sup> Derived *H<sub>v</sub>* in Vickers scale = 92.65 × nanoindentation hardness *H* (GPa) [14].

a larger workability index is achieved. The cast composites were cut into pieces of rectangular cross sections with an initial height of 10 mm as well as 12 mm. Table 2 shows the workability index for cold rolled specimens of three types of composites.

In case of cold rolling at ambient temperature, all the composites were initially deformed approximately by 10% (height reduction), which resulted a workability index of 1.1. Then the composites were thinned down to maximum possible reduction without fracture. The maximum reduction was carried successfully with a WI of 2 without any cracking for 2 wt% Al<sub>2</sub>O<sub>3</sub> reinforcement. With increase in the particles wt% in the composite, cold workability decreased as indicated by reduced WI, in Table 2. Composite with 3.57% reinforcement produced a maximum WI of 1.75 whereas, 1.41 (max) WI was obtained for 4.69% reinforced composite. Increase in the particle concentration in the matrix reduces the strain accumulation capability of the matrix during plastic deformation. Therefore, geometric work-hardening during densification by higher volume fraction of reinforcement and matrix work-hardening during cold deformation led to reduce the ductility of the higher particles reinforced material [15].

A spatial parameter of great importance in the particulate system is the mean free-distance or inter-particle spacing ( $\lambda$ ) between the particles. As defined by Fullman [16]

$$\lambda = \frac{1 - (V_V)_p}{N_L} \quad (1)$$

where  $(V_V)_p$  refers to the volume fraction of particles in the composite and  $N_L$  is the number of intercepts per unit length of test lines with the particles. Eq. (1) is valid regardless of size, shape, or distribution of particles. The detailed analysis of inter-particle spacing has been described in somewhere [12]. The estimated inter-particle spacing ( $\lambda$ ) obtained micrographs is 24 nm [12]. Alternatively, if uniformly sized Al<sub>2</sub>O<sub>3</sub> particles of 10 nm diameter are assumed to be equi-spaced in the Al matrix and volume fraction of Al<sub>2</sub>O<sub>3</sub> within the composite is taken as 0.05, inter-particle separation distance turns out to be 21.8 nm. Therefore, theoretically calculated inter-particle spacing is very close to the actual value estimated from the micrographs [12].

The Orowan stress ( $\tau_{or}$ ) could be estimated from the relation [11]

$$\tau_{or} = Gb/\lambda \quad (2)$$

where,  $G$  is the shear modulus,  $b$  is Burgers vector and  $\lambda$  is the average inter-particle spacing. Since  $G$  for cp-Al = 27.5 GPa [11],  $b = 0.286$  nm [11] and calculated inter-particle distance = 24 nm, the  $\tau_{or}$  would be 327.7 MPa for 2% Al<sub>2</sub>O<sub>3</sub> composite. The required stress would be more for higher Al<sub>2</sub>O<sub>3</sub> reinforced composites as the inter-particles distance would be less.

As the particle concentration increases inter-particle spacing is reduced. Therefore, a higher stress is required to overcome the obstacle by the dislocation. Therefore, the workability of the

particle reinforced material decreases with increasing particle concentration as dislocation movement is hindered by more number of particles in higher particle reinforced material. Moreover, in the higher particle reinforced materials, there is a chance of particles agglomeration and clustering. So, a non-uniform particles distribution leads to pre-mature cracking of material during cold working. Therefore, workability reduces [6].

Increasing the temperature increases ductility of the composite, thereby increases its workability. But, increasing temperature after certain limit results in grain coarsening leading to decrease in the mechanical properties of the composite. Therefore, the mechanical properties of composite can be optimized through a controlled thermo-mechanical treatment. Table 3 shows the workability index for hot rolled composites with different wt% of reinforcement. Hot rolling of the present nanocomposites was carried out successfully at 300 °C after soaking for 1 h at 350 °C with a maximum WI of 8 for 2%, 7 for 3.57% and 6 for 4.69% reinforcement, respectively. Like cold rolling here also it was seen that maximum workability of the composite decreased with increasing wt% of reinforcement. Higher the volume fraction of the reinforcement for a particulate size, more number of obstacles is to be bypassed by the dislocation and easily work-hardened the matrix. Although, dynamic recrystallization favors strain relaxation in Al matrix to some extent at 0.6  $T_M$  (where,  $T_M$  is the melting point in K), the workability of the composite decreases with increasing volume fraction of the reinforcement because of geometric work-hardening due to particle concentration and matrix work-hardening due to strain concentration [15].

Fig. 6 shows the variation of reduction ratios of the cold and hot rolled Al–Al<sub>2</sub>O<sub>3</sub> nanocomposites with increase in the percentage of reinforcement. Although % drop in WI are nearly equal for cold and hot rolling due to increase in the reinforcement from 2 wt% to 3.57 wt%, the absolute values of cold WI and hot WI were differ by a factor of ~4. The values of WI are expected to dependent on the fracture mechanisms operative at the corresponding temperature, which was not taken up for the present investigation.

Table 4 reports the effect of cold and hot rolling of Al–2% Al<sub>2</sub>O<sub>3</sub> composite on elastic modulus and hardness. Reinforcement with 2% Al<sub>2</sub>O<sub>3</sub> resulted in ~3.6% increase in the elastic modulus than the ultrasonically cast cp-Al as discussed earlier. Cold working of the composite increased the elastic modulus by 7% with a maximum WI of 2, whereas, hot rolling of same composite at 300 °C showed an improvement of elastic modulus with increasing WI. The maximum value of elastic modulus was 80.6 GPa obtained for the hot rolled composite with a maximum WI of 8. The elastic modulus of the metals and alloys is not quite sensitive to the structural features changed by rolling like grain size, point defects and dislocation density etc. [11]. Therefore, the enhancement of elastic modulus by cold and hot rolling was possibly due to the increased in the relative density and/or changed in the

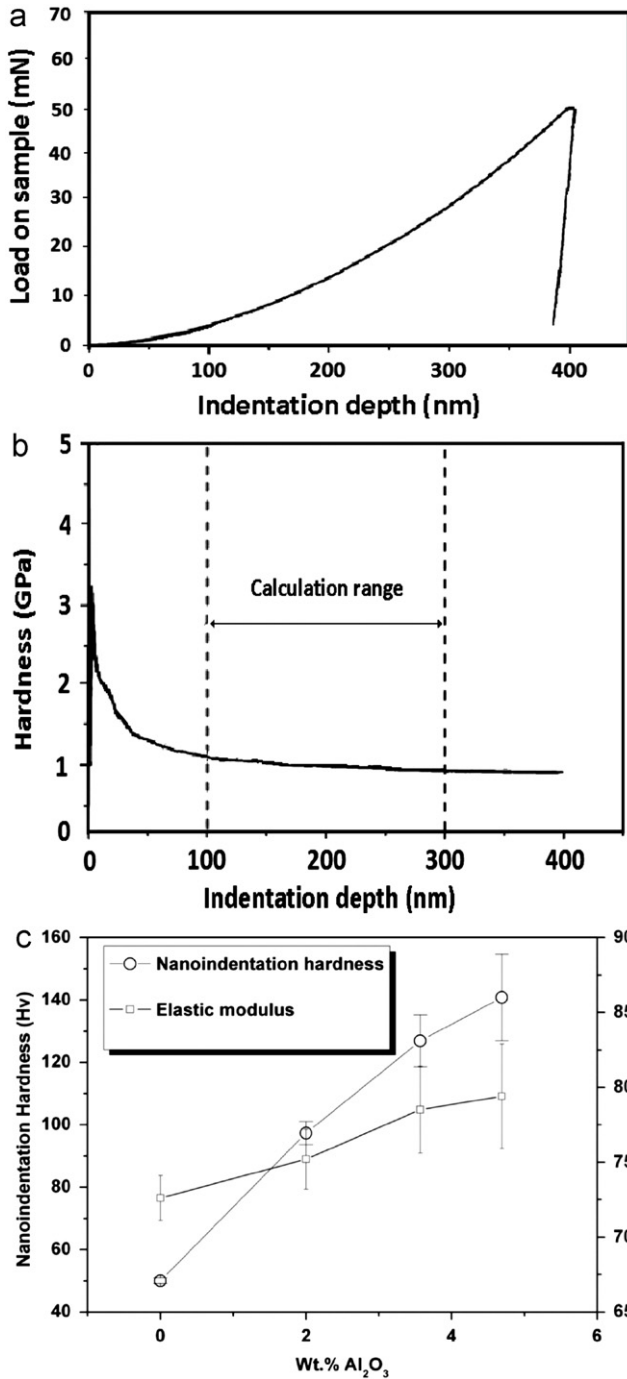


Fig. 3. (a) Typical load-displacement curve and (b) hardness vs. displacement plots during nanoindentation tests on Al-2% Al<sub>2</sub>O<sub>3</sub> nanocomposite. (c) Variation of nanoindentation hardness and elastic modulus of Al-Al<sub>2</sub>O<sub>3</sub> nanocomposites with increase in the reinforcement.

morphology of the microstructure of the composites. The statistical data of the elastic modulus measurement from 40 locations showed more uniform results for hot rolled composites than the as-cast and cold rolled materials. This was possibly because of redistribution of the particulates more uniformly during the formation recrystallized grains by dynamic recovery and recrystallization processes during hot rolling of the composites.

2% Al<sub>2</sub>O<sub>3</sub> reinforcement in cp-Al matrix resulted in ~100% enhancement of hardness values (Table 4). Cold rolling of the composite up to a WI of 2 resulted in further enhancement of the

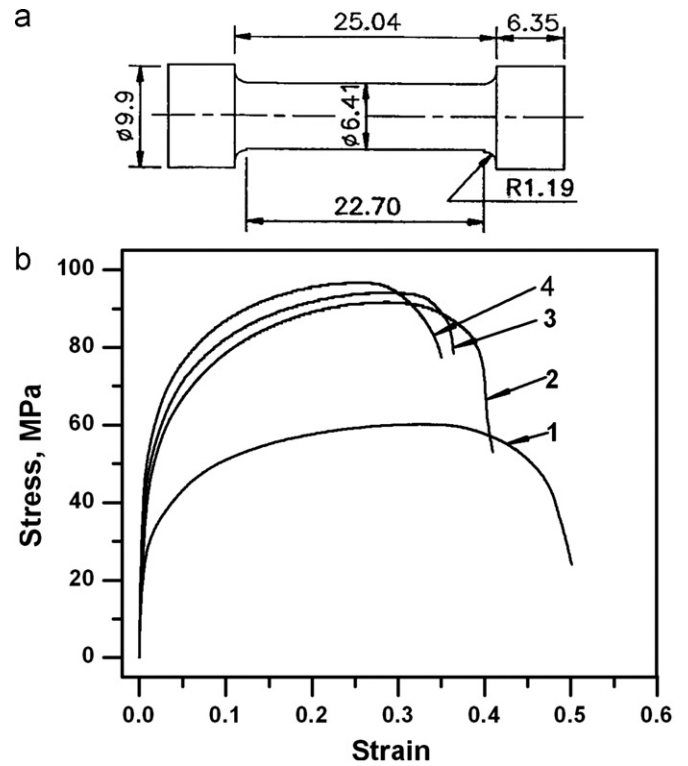


Fig. 4. (a) Tensile specimen drawing as per ASTM E8 standard (all dimensions in mm) and (b) comparison of engineering stress-strain curves of (1) cp-Al, (2) Al-2% Al<sub>2</sub>O<sub>3</sub>, (3) Al-3.57% Al<sub>2</sub>O<sub>3</sub> and (4) Al-4.69% Al<sub>2</sub>O<sub>3</sub> nanocomposites.

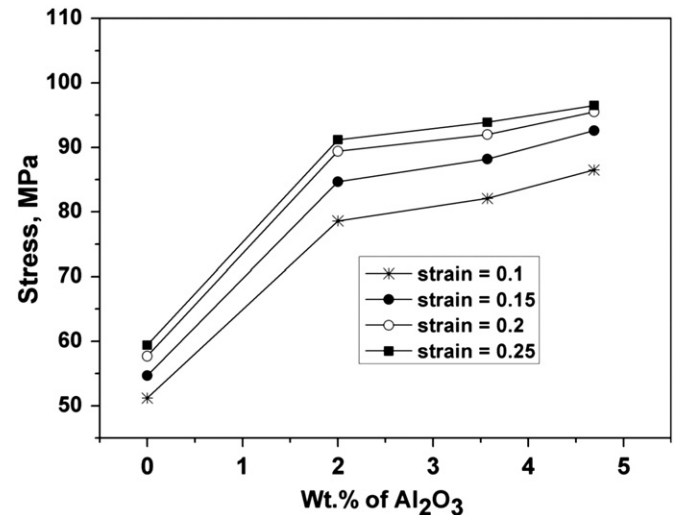


Fig. 5. Engineering stress vs. wt% of reinforcement in Al-Al<sub>2</sub>O<sub>3</sub> nanocomposites at various strains.

Table 2  
Workability index (WI) of cold rolled Al-X% Al<sub>2</sub>O<sub>3</sub> composites.

Reinforcement wt%	Initial height (H <sub>0</sub> ) (mm)	Final height (H) (mm)	Workability index (H <sub>0</sub> /H)
2	10	9	1.1
	10	5	2.0 (max)
3.57	10	9	1.1
	10	5.7	1.75 (max)
4.69	10	9	1.1
	10	7.1	1.41 (max)

hardness values by 40–50% due to increase in dislocation density. Hot rolling at 300 °C with a WI of 2 showed a hardness value of 80.6  $H_v$ . With increased WI, the hardness values also increased and a maximum value of 112  $H_v$  was obtained for a hot WI of 8. The initial reduction of the hardness value of the hot worked specimen compared to that of the as-cast composite was possibly due to annihilation of thermal stress and grain coarsening during soaking at 350 °C for 1 h. The coarse grained material possibly was not recrystallized by dynamic recovery and recrystallization processes during a small (elapsed) duration of hot rolling with a WI of 2. With increased WI sufficient time was obtained for dynamic recovery and recrystallization to take place and recrystallized fine grained composite was formed with more uniform distribution of particulates. Therefore, strengthening of the hot rolled composite was due to two reasons; grain refinement by dynamic recovery and recrystallization processes, and from

redistribution of fine particles by the thermo-mechanical treatment. There was a good similarity between the average nanoindentation hardness, microhardness and Vickers hardness measurement for each type of specimen as shown in Table 4. The more uniform structure could be ascertained from the statistical data of the nanoindentation hardness measurement (Table 4). The standard deviation data was much less for hot worked specimen for a WI of 8 compared to that of the as-cast or cold worked composites. This certainly indicates that the particulates were more uniformly distributed in the matrix than that of the as-cast specimen.

Fig. 7(a) and (b) displays the effect of cold and hot rolling on elastic modulus and hardness of Al–2%  $Al_2O_3$  nanocomposite. In the insets of these figures, the variation of standard deviations (also shown in Table 4) clearly showed that the hot rolling

**Table 3**  
Workability index (WI) of hot rolled Al– $Al_2O_3$  composites.

Reinforcement wt%	Initial height ( $H_0$ ) (mm)	Final height ( $H$ ) (mm)	Workability index ( $H_0/H$ )
2	12	6	2
	12	3	4
	12	1.5	8 (max)
3.57	12	6	2
	12	3	4
	12	1.7	7 (max)
4.69	12	6	2
	12	3	4
	12	2	6 (max)

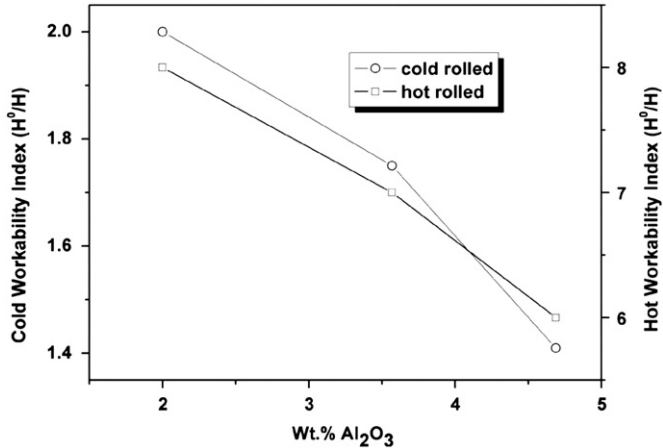


**Fig. 6.** Cold and hot workability index (WI) of Al– $Al_2O_3$  nanocomposites with increase in the reinforcement.

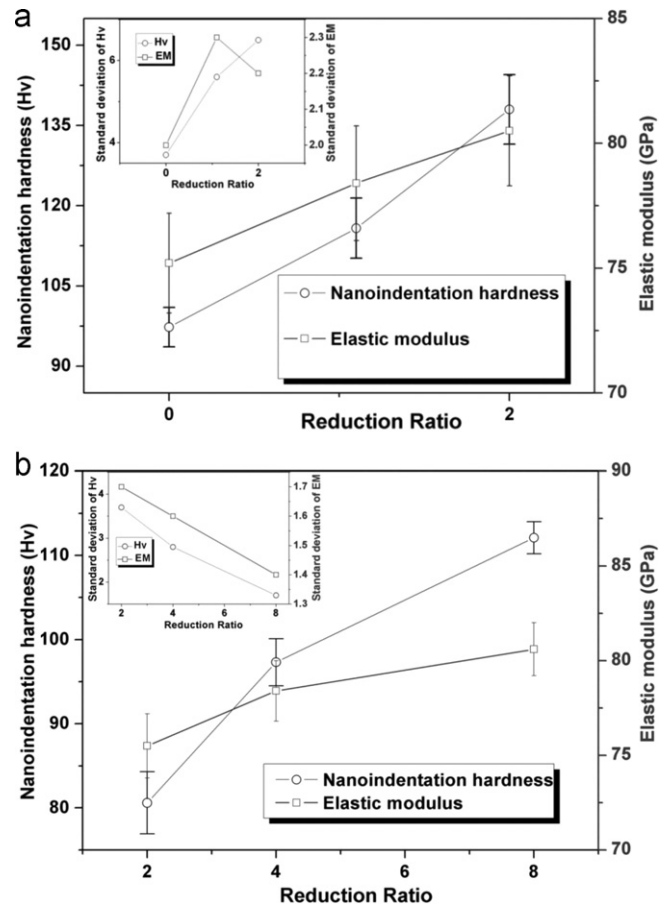


**Fig. 7.** Effect of (a) cold and (b) hot rolling on elastic modulus and hardness with increase in the reduction ratio of Al–2%  $Al_2O_3$  nanocomposite.

**Table 4**  
Effect of cold and hot rolling of Al–2%  $Al_2O_3$  composite on elastic modulus and hardness.

	As-cast	C.R. <sup>a</sup> at room temperature		H.R. <sup>b</sup> at 300 °C after soaking at 350 °C for 1 h		
Workability index (WI) ( $H_0/H$ )	–	1.1	2	2	4	8
Nanoindentation						
Elastic modulus $Y$ (GPa)	75.2 ± 2.0	78.4 ± 2.3	80.5 ± 2.2	75.5 ± 1.7	78.4 ± 1.6	80.6 ± 1.4
Nanoindentation hardness $H$ (GPa)	1.05 ± 0.04	1.25 ± 0.06	1.48 ± 0.07	0.87 ± 0.04	1.05 ± 0.03	1.21 ± 0.02
Derived $H_v$ (from $H$ value <sup>c</sup> in GPa)	97.3	115.8	137.1	80.6	97.3	112.1
Vickers hardness ( $H_v$ )	102.0	118	139	81	96	113
Microhardness ( $H_v$ )	100.0	119	138	85	99	112

<sup>a</sup> C.R. stands for cold rolling.

<sup>b</sup> H.R. stands for hot rolling.

<sup>c</sup> Derived  $H_v$  in Vickers scale = 92.65 × nanoindentation hardness  $H$  (GPa) [14].

(Fig. 7(b)) resulted in more uniform distribution of the nano-sized  $\text{Al}_2\text{O}_3$  particles, while the cold rolling increased the heterogeneity with increase in the reduction ratio (Fig. 7(a)).

#### 4. Conclusions

- (1) Nearly 57% increase in the tensile yield strength was obtained in the present Al–2%  $\text{Al}_2\text{O}_3$  nanocomposite, as compared to those of the commercially pure (cp) Al, cast by the NCUC method. Increase in the  $\text{Al}_2\text{O}_3$  beyond 2 wt% did not result in significant increase in the yield strength, possibly because of agglomeration and non-uniform distribution of nanosize  $\text{Al}_2\text{O}_3$  particles beyond 2 wt%.
- (2) Approximately 92% increase in the microhardness and ~94% increase in nanoindentation hardness were resulted for Al–2%  $\text{Al}_2\text{O}_3$  nanocomposite, compared to that of the ultrasonically cast cp-Al. The hardness of the nanocomposites increased with increase in the reinforcement, which also increased the heterogeneity of the structures. The standard deviation values in the nanoindentation hardness and elastic modulus for the as-cast nanocomposites were higher than those in the ultrasonically cast cp-Al, indicating the increase in sub-micron levels heterogeneity of the structures.
- (3) Cold and hot rolling revealed that the nanocomposites were significantly workable and the workability was reduced with increase in the weight percentage of reinforcement.

#### References

- [1] I.A. Ibrahim, F.A. Mohammed, E.J. Lavernia, *J. Mater. Sci.* 26 (1991) 1137–1155.
- [2] K.K. Chawla, P.K. Liaw, S.G. Fishman, *J. Manage.* 48 (2) (1996) 43–44.
- [3] J.U. Ejiolor, R.G. Reddy, B.A. Okorie, *J. Mater. Sci.* 33 (1997) 1003–1013.
- [4] J.U. Ejiolor, R.G. Reddy, *J. Manage.* 49 (1997) 31–37.
- [5] Mohamed A. Taha, Nahed A. El-Mahallawy, Ahmed M. El-Sabbagh, *J. Mater. Process. Technol.* 202 (2008) 380–385.
- [6] K. Akio, O. Atsushi, K. Toshiro, T. Hiroyuki, *J. Jpn. Inst. Light Met.* 49 (1999) 149–154.
- [7] K.M. Mussert, W.P. Vellinga, A. Bakker, S. Van Der Zwaag, *J. Mater. Sci.* 37 (2002) 789–794.
- [8] J. Lan, Y. Yang, X. Li, *Mat. Sci. Eng. A* 386 (2004) 284–290.
- [9] Y. Yang, J. Lan, X. Li, *Mat. Sci. Eng. A* 380 (2004) 378–383.
- [10] P. Padhi, *Experimental and Theoretical Studies on Particle Distribution in Cast Aluminum-Based Metal Matrix Composites*. Ph.D. Dissertation at I.I.T., Kharagpur, 2007.
- [11] G.E. Dieter, *Mechanical Metallurgy*, McGraw Hill Book Company (UK), London, 1988, pp. 49, 154–155, 208–209, 217–220, 280–281, 503–505, 526–529.
- [12] S. Mula, P. Padhi, S.C. Panigrahi, S.K. Pabi, S. Ghosh, *Mater. Res. Bull.* 44 (2009) 1154–1160.
- [13] N.K. Mukhopadhyay, P. Paufler, *Int. Mater. Rev.* 51 (2006) 209–245.
- [14] M.T.S. System Corporation (1999–2002), *MTS-XP Test Works Manual 2001*, Version no. 16, pp. 391–392.
- [15] R. Narayanasamy, V. Anandakrishnan, K.S. Pandey, *Mater. Des.* 29 (2008) 1582–1599.
- [16] R.L. Fullman, *Trans. AIME* 197 (1953) 447–452.